Analytical Chemistry Research 3 (2015) 54–62

Contents lists available at ScienceDirect

Analytical Chemistry Research

journal homepage: www.elsevier.com/locate/ancr

Analysis of cave atmospheres by comprehensive two-dimensional gas chromatography (GC×GC) with flame ionization detection (FID)

Ryan C. Blase *, Edward L. Patrick, Joseph N. Mitchell, Mark Libardoni

Southwest Research Institute, 6220 Culebra Road, San Antonio, TX 78238, United States

ARTICLE INFO

Keywords:
Cave atmospheres (speleology)
Comprehensive two-dimensional gas chromatography (GC×GC)
Environmental sampling
Multi-bed sorption trap

ABSTRACT

In this paper, we describe a simple method for sampling, pre-concentrating, and separating volatile and semi-volatile components from two different cave atmospheres. Sampling is performed by capturing a volume of cave atmosphere in a Tedlar bag or Suma canister for sample storage and transport back to the laboratory. Loading a portion of the sample on a multi-bed sorption trap allows for sample pre-concentration prior to separation and detection of components on a comprehensive two-dimensional gas chromatograph (GC×GC). Comparison of two Texas caves reveals the power of comprehensive two-dimensional gas chromatography (GC×GC) for volatile separation and detection, and to our knowledge marks the first use of GC×GC for the analysis of cave atmospheres. Analysis of the results revealed 138 and 146 chromatographic signals over an S/N threshold of 500 and direct comparison of the two samples revealed 50 identical chromatographic signals. This study is a first step toward demonstrating the ability of GC×GC to separate the complex volatiles and semi-volatiles in the cave atmosphere as a fingerprinting tool.

1. Introduction

A number of recent discoveries have triggered renewed interest in cave environments. Among these was the discovery of extremophile bacteria in Cueva de Villa Luz in Mexico that metabolize minerals and hydrocarbons while living in concentrated sulfuric acid (pH 0.0) [1,2]. Caves also entered the realm of the extraterrestrial when their presence was detected on the surface of Mars by the NASA Mars Odyssey orbiter's Thermal Emission Imaging System (THEMIS) in 2007 [3]. Perhaps the most pressing current issue involving cave environments was the discovery in 2006 of the highly-infectious and rapidly-spreading fungal disease known as "white nose syndrome" (WNS) among bats in Schoharie County, New York, and traced to the psychrophilic fungus *Pseudogymnoascus destructans* [4–6]. WNS has now spread to over a dozen U.S. states and several Canadian provinces, and claimed an estimated 5.6 million bats [7]. Studying the atmospheres of these complex and diverse environments not only serves as a diagnostic aid in understanding extremes in the boundary conditions of terrestrial microbes, but also has implications for astrobiology [8] and the origins of life on Earth [9].

Over the past five years, members of our experienced cave team have conducted studies of the changing meteorological conditions in caves in the vicinity of San Antonio, Texas. This work involved continuous logging of temperature, barometric pressure, humidity, airflow, and carbon dioxide levels [10]. This cave microclimate work was further expanded in 2011 in a collaboration between St. Mary's University and Southwest Research Institute (SwRI) to deploy a cave mass spectrometer (CMS) in four Texas caves, including Bracken Bat Cave, home to the largest colony of maternity bats in the world. Discrete air samples were also obtained in Bracken for subsequent analysis at SwRI by gas chromatograph mass spectrometry (GCMS).

The air samples for Bracken Bat Cave were obtained during peak occupation of the colony when the interior temperature of the cave was 43.3 °C and humidity greater than 99%. Subsequent analysis revealed a complex mixture of organic molecules that included hydrocarbons, ketones, aldehydes and alcohols, as well as compounds that could not be identified against the background noise of overlapping chemical signatures. A more powerful analytical chemistry method was essential to unravel the mysteries of such a harsh and complex natural environment teeming with life. To the best of our knowledge and despite its limitations, this effort to characterize cave atmospheres by GCMS was also the first of its kind. Details of that effort have been described previously [11].

* Corresponding author. Tel.: +1 210 522 5638; fax: +1 210 522 4678.
E-mail address: rblase@swri.edu (R.C. Blase).

http://dx.doi.org/10.1016/j.ancr.2014.09.002
2214-1812/

It is rare for caves in South Texas to experience freezing temperatures even in winter, so these caves are not known to contain the fungus that causes WNS. Even so, colonies of the fungus responsible for WNS have been shown to grow well at temperatures between 0 and 15 °C, poorly at temperatures between 15 and 20 °C and not at all at higher temperatures [12]. Also, bats in maternity colonies in South Texas do not exhibit the depressed or compromised immune systems characteristic of bats in torpor within hibernacula in colder climates where WNS is prevalent. However, warm cave environments do serve as complex biological and environmental analogues for conditions encountered in colder North American caves afflicted by WNS. Texas caves can also serve as field laboratories for the deployment of analytical techniques and testing protocols that can also be used in infected caves, yet without the same program constraints that arise in WNS-afflicted regions due to contamination concerns. Furthermore, the inventory of atmospheric volatiles within the air of hot and humid South Texas caves is anticipated to be far more complex than similar volatiles encountered at the reduced temperatures within caves in the Northeast.

Comprehensive two-dimensional gas chromatography, more commonly referred to as GC×GC, has become a powerful analytical tool since its inception [13–15]. In 1991, Phillips et al. developed the first comprehensive GC×GC which employed a thermal modulator for transferring effluent from the first column to the second column [16]. This novel technique of GC×GC has allowed the separation and analysis of complex samples such as petroleum [17–19], flavors [20], metabolites [21–23], environmental [24,25] and even human breath [26]. The technique of GC×GC employs two serially coupled capillary columns of different selectivity via a modulation device. The modulator continuously traps and re-focuses the first column effluent and subsequently injects it onto the second column for a rapid analysis. This continuous process allows the entire sample to undergo separation on both columns. In a non-polar (*x*) polar column configuration, the first column separates components based on volatility, similar to one-dimensional separation, while the second column separates components by a different physical characteristic, in this example by polarity (also similar to a one-dimensional separation). The second dimension separation is very fast, on the order of a few seconds, meaning that analysis time is virtually unchanged from 1-dimensional GC.

The analytical advantages of GC×GC are multiple. First, the focusing of eluting bands from the first dimension in the thermal modulator and re-injection of the focused band onto the second dimension column results in improvements in both signal-to-noise (S/N) ratios and detectability (providing lower limits of detection). The higher amplitude, narrow peak widths provided from thermal modulation provide increased chromatographic resolution. Furthermore, the two-dimensional separation allows for the data to be presented on a two-dimensional retention plane rather than a single dimension (chromatogram). The two-dimensional retention plane provides visual evidence of the increase in peak capacity; the total peak capacity being the product of each single dimension peak capacity. Trend lines reveal chemical family recognition, or groupings of chemical families within the two-dimensional retention plane. The analytical advantages of GC×GC and its impact in separation science are well documented in review articles [27,28].

Armed with the knowledge that caves are a complex habitat for extremophile microbes, that an epidemic is killing bats directly tied to their natural cave environment, and that caves are on Mars, we sought to apply the GC×GC separation technique as an analytical chemistry tool for fingerprinting this complex environment. This application is tested by comparing the fingerprints of two separate cave environments.

2. Experimental

2.1. Cave sampling

Cave atmospheric samples were acquired by investigators descending into caves to obtain air samples from just above the floor in a deep interior portion of each cave (samples were taken just above the floor for the sake of simplicity, it is possible that the atmospheric profile may change at different strata in the cave). The sample container used for collection and storage was either a 1 L Tedlar bag or an evacuated 1 L Suma canister. Each of these types of sample containers has advantages and disadvantages [29]. In its deflated sampling configuration, the Tedlar bag is square in shape and very small when compared to a Suma canister. Constructed from heavy-duty plastic, the bag is inflated by a tracheal syringe to an internal volume of 1 L through a quarter-turn valve. Thus, a 1 L tracheal syringe is used to first sample the atmosphere and then the sample is expelled from the syringe into the Tedlar bag. The quarter turn valve on the bag is then closed and the sample returned to the laboratory for analysis. Perhaps even easier sampling is accomplished through use of a Suma canister. The Suma canister is evacuated by a vacuum pump (to 30 psi below atmospheric pressure) prior to descent into the cave. Once in the cave sampling location, the valve on the canister is simply opened and the local atmosphere is drawn into the canister until the pressure equilibrates, a procedure that takes less than two seconds. The valve is then returned to the closed position and the canister returned to the laboratory for analysis. An advantage of the Suma canister is its ruggedness, structural rigidity, and the stainless steel inner surface walls. The durability of the sample container can be a critical issue during lengthy cave descents and ascents in which Tedlar bags could be perforated against rock while negotiating tight spaces. The structural rigidity of the Suma canister also allows pressurization with helium if desired once returned to the laboratory. The size and mass of the Suma canister limits the number of samples that can be retrieved on a typical cave expedition. The unfilled Tedlar bags are compact and can be carried through tight spaces, but still require the time and effort associated with the large sampling syringe for filling. The inner walls of the Suma canister are also less reactive than walls of the Tedlar bags, which are subject to permeation and other surface effects related to gas reactivity and retention. For this study, a sample was taken from a cave in the western part of Texas while the other sample was taken from Robber Baron cave in San Antonio. Both samples were returned to Southwest Research Institute for analysis in the GC×GC lab of the Space Science and Engineering Division. Cave samples were taken on expeditions into caves by employees from Southwest Research Institute and were taken with permission from cave managers or land owners where the cave was present. For this reason, only a limited number of samples could be taken. Temperature and humidity measurements of the cave were not taken at the time of sampling and while these data could have provided additional information, for the purpose of this experiment showing the analytical utility of GC×GC for investigating cave atmospheres are not required.

2.2. Pre-concentration with multi-bed sorption trap

Upon return to the laboratory, the sample container was connected to a multi-bed sorption trap where sample pre-concentration, or enrichment, is accomplished prior to injection on a GC×GC commercial instrument. The multi-bed sorption trap (MBST) consists of four discrete beds of carbon molecular sieve material separated by plugs of glass wool. The carbon molecular sieve materials are as follows: Carbopack Y, Carbopack X,

Carbopack B, and Carboxen 1000 (Supelco; St. Louis, MO). Each bed component, surface area size, and relative analyte size trapped in the bed (related to hydrocarbon size) are displayed in Table 1. The beds are packed within a thin walled Inconel 600 tube (8 cm length, outer diameter of 0.0625″ (1/16″), with a wall thickness of 0.006″ from AllTube Microgroup; Medway, MA), allowing for quick resistive heating of the trap to desorb components into the comprehensive two-dimensional gas chromatograph. Details, applications, and performance of the multi-bed sorption trap have been published previously [26,30,31].

A schematic of the sample pre-concentration and subsequent analysis step in the GC×GC instrument is displayed in Fig. 1. Sample is drawn from the sampling container (sampling pathway is denoted by the dotted maroon line in the figure), a Suma canister in the figure, with a diaphragm vacuum pump (S/N 1/667418 KNF Neuberger Inc.; Trenton, NJ). During sampling, the valve for the sample inlet is opened and the two-way valve is switched to open the plumbing to the vacuum pump. Valve control is accomplished through a Crydom D1D40 solid state relay (Digi-Key Corporation; Thief River Falls, MN). A flow controller (Omega Engineering Model FMA.5605, Omega Engineering; Stamford CT) is placed upstream from the vacuum pump so the vacuum flow rate is known and the time duration of sampling along with the known flow rate can be used to calculate the volume of gas sampled from the container. The sample is collected on the trap with each analyte being trapped on a respective bed according to its size with larger analytes being trapped on the first bed (lower volatility components) and smaller analytes (higher volatility components) trapped on the last beds. All plumbing between the valves, the MBST, and the GC×GC is accomplished by using an Rxi guard column of inner diameter 250 μm (Restek Corporation; Bellefonte, PA).

After a user-defined sampling period, the sample inlet valve is closed and the two-way valve is switched to allow helium carrier gas to flow through the trap and the GC×GC columns. Time is allowed for carrier gas equilibration through the entire set-up before desorption of components off the trap and injection onto the primary column of the GC×GC instrument. Carrier gas flow is defined by the dotted olive green line in the figure.

Upon helium carrier gas equilibration, a relatively fast, high-current DC heating pulse is applied across the multi-bed sorption trap (Inconel 600 tube) followed by a second, lower-current DC heating pulse to maintain the MBST temperature. The first heating pulse is a 3.8 V DC (~17.5 A) pulse of 2.5 second duration, followed by a 1.4 V DC (~6–7 A) pulse of 15 s duration. The MBST is heated to 300 °C during the initial pulse and temperature is maintained around this maximum temperature from the second heating pulse. Control of the heating pulses are accomplished by two, separate Crydom D1D40 solid state relays with an Agilent E3633A DC power supply (0–8 V, 20 A/0–20 V, 10 A) for the first heating pulse and an Agilent E3634A DC power supply (0–25 V, 7 A/0–50 V, 4 A) for the second heating pulse delayed 0.2 s after the fall of the first heating pulse (Agilent Technologies; Santa Clara, CA). MBST temperature is monitored by a TT-K-40 fine wire duplex insulated thermocouple (Omega Engineering; Stamford, CT) with the thermocouple wire attached to the middle surface between the heating contact points and the thermocouple wire is fed into a model DP116-KC1 temperature panel meter (Omega Engineering; Stamford, CT). Coinciding with the rise of the first heating pulse is the manual start of the GC×GC (pseudo-injection on the GC×GC) for analysis of the desorbed components. Retention time shifts between replicate runs was seen to be less than 4 s in the first dimension (corresponding to the GC×GC modulation time). Random selection of five chromatographic signals were compared for triplicate runs and all of them showed the first dimension retention time to be "dead on" while the second dimension retention time shifted by only ±0.015 s.

All of the timing for valve operation and heating pulses is accomplished through a LabVIEW (National Instruments; Austin, TX) program custom-written by the authors. Valve signals and heating pulse signals are relayed out of digital-out signals on a National Instruments USB-6009 DAQ (National Instruments; Austin, TX) while the temperature of the MBST is fed back into an analog input on the DAQ and stored in a plot in the LabVIEW program. This program allows experimental parameters to be easily changed or for reproducibility between multiple experimental runs when experimental values are kept constant.

All other pertinent experimental parameters associated with sample loading for the samples presented herein are described

Table 1
Bed component, surface area size of component and relative analyte size trapped.

Bed component	Surface area size (m^2/g)	Relative analyte size trapped
Carbopack Y	24	C_{12}–C_{20}
Carbopack B	100	C_5–C_{12}
Carbopack X	240	C_3–C_9
Carboxen 1000	1200	C_2–C_5

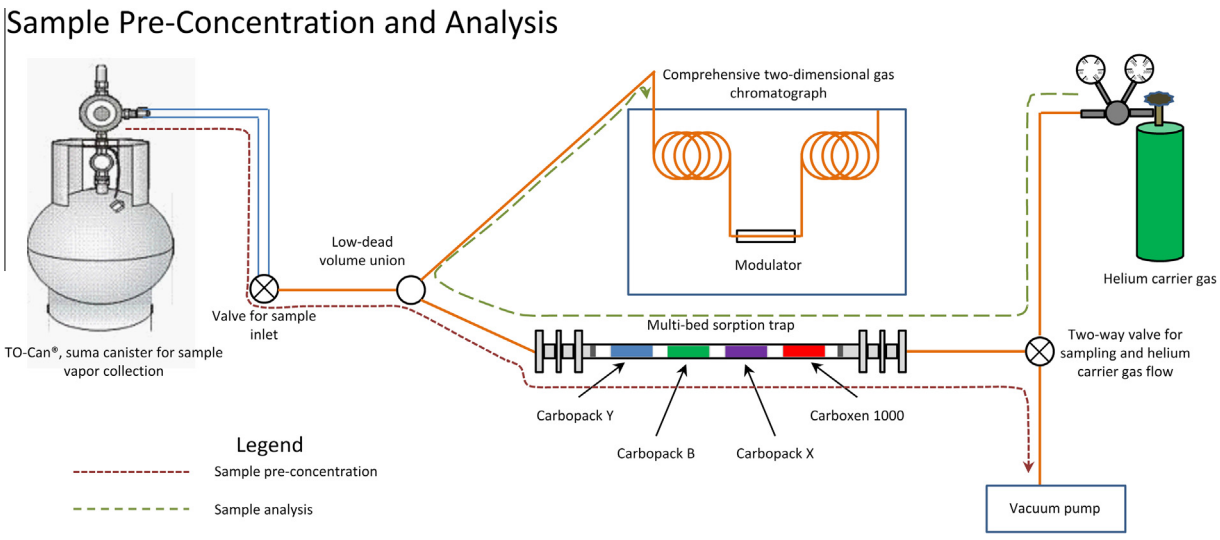

Fig. 1. Schematic of sample pre-concentration on multi-bed sorption trap and analysis via GC×GC.

below. Sample was loaded onto the MBST for 50 s and the flow rate onto the trap provided from the vacuum pump and measured by the flow meter was approximately 40 ml min^{-1}. Thus, approximately 33.3 ml of gas was loaded onto the MBST for each run with the experiment being done in triplicate. After sample loading, the two-way valve was switched to allow helium carrier gas to flow through the MBST and GC×GC instrument for 300 s to permit equilibration of flow and pressure throughout the whole system. After this time period, the two heating pulses were turned on and the desorbed components were analyzed by the GC×GC instrument.

Between runs, the trap is conditioned by purging helium gas through the trap while maintaining trap temperature at about 150–200 °C. In this way, any remaining trapped components from the previous run will be desorbed from the trap. This conditioning process ensures that the trap is clean prior to the next run.

2.3. Comprehensive two-dimensional gas chromatograph (GC×GC)

The comprehensive two-dimensional gas chromatograph (GC×GC, Leco Corporation; St. Joseph, MI) is an Agilent 7890 GC (Palo Alto, CA) equipped with a consumable free thermal modulator and flame ionization detector (FID). The instrument is slightly modified to allow for the MBST to be mounted near the GC inlet. Modifications include removal of the autosampler, removal of the inlet liner, and helium carrier gas flowing directly through the trap and through the GC×GC columns rather than using the electronic pressure controller of the instrument. To accomplish this, the Rxi guard column (250 μm id) exiting the low-dead volume connector to the GC inlet passes through the inlet and into the oven and is connected to the primary dimension column by way of a Universal Press-Tight® connector (Restek Corporation; Bellefonte, PA). The carrier gas flow rate was measured with the GC oven at an isothermal temperature of 30 °C and was set to a flow rate of 1.5 ml min^{-1} and used for all experiments described herein. For all experimental data shown, the inlet temperature was 250 °C.

The columns used in the GC×GC instrument are a 30 m long, 250 μm id, 0.25 μm film thickness Rtx-1 primary column and a 1.3 m long, 100 μm id, 0.1 μm film thickness Rxi-17 secondary column (Restek Corporation; Bellefonte, PA). The oven temperature program ramps are as follows: primary oven 40 °C hold for 0.5 min followed by a 3 °C min^{-1} ramp to 240 °C held for 0.5 min and secondary oven 50 °C hold for 0.5 min followed by a 3 °C min^{-1} ramp to 250 °C and then held for 0.5 min at the final temperature. The modulator temperature is held 15 °C above the secondary oven temperature over the entire course of the run. The two-stage modulator period is 4 s (1.4 s cold pulse and 0.6 s hot pulse of gas for each stage), defining the overall retention time of the second dimension. The instrument employs a flame ionization detector (FID) which provides a signal response, or current, for analytes eluting from the secondary column. Data were post-processed with the ChromaTOF® software (Leco Corporation; St. Joseph, MI).

3. Results and discussion

The first sample to be run was taken from the cave in western Texas herein referred to as BBC cave. The sample was captured in a 1 L Tedlar bag and was brought back to the laboratory and analyzed within 4 days of the sample being taken. The experiments were done in triplicate and the heating profiles of the MBST for the three runs are displayed in Fig. 2. It can be seen from Fig. 2 that the time of heating (desorption of components from the trap) and the temperature of the MBST versus time shows good reproducibility between the experimental runs. Similar results were seen for the other cave samples but the data are not shown for reasons of brevity and simplicity.

The sample components then undergo separation on both the primary and secondary dimension column and with the analytical advantages of the thermal modulator the chromatographic signals are narrow and of increased sensitivity. A two-dimensional contour plot (chromatogram) of the chromatographic signal intensity versus first and second dimension retention time is shown in Fig. 3. For clarification purposes, the important parts of the figure to call out are the first dimension retention time (*x*-axis), the second dimension retention time (*y*-axis), and the contour plot (color scheme) is blue for the background noise, then green-to-yellow-to-red in terms of increasing chromatographic signal intensity. The signals standing out from the background show all of the chromatographic signals (volatile and semi-volatile substances) present in the atmospheric cave sample, 138 chromatographic signals above an S/N threshold of 500 on average between the three triplicate experimental runs. The S/N threshold was chosen to examine similarity in higher abundance components that can be seen more easily from the two-dimensional plots. If the S/N threshold was reduced to lower values, for example around an LOD of 10, the number of identified chromatographic signals would increase. This large number of chromatographic signals demonstrates the complexity of the sample. The streaking of signal in the early first dimension retention times is due to the high volatility of the corresponding compound and the cold gas jet temperature of the

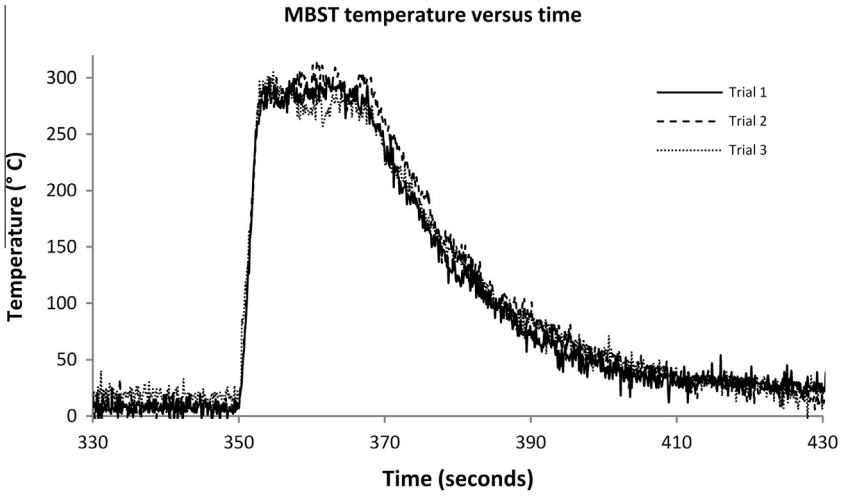

Fig. 2. Temperature profile of the MBST during heating. The first heating pulse begins at 350 s from the beginning of the trap loading.

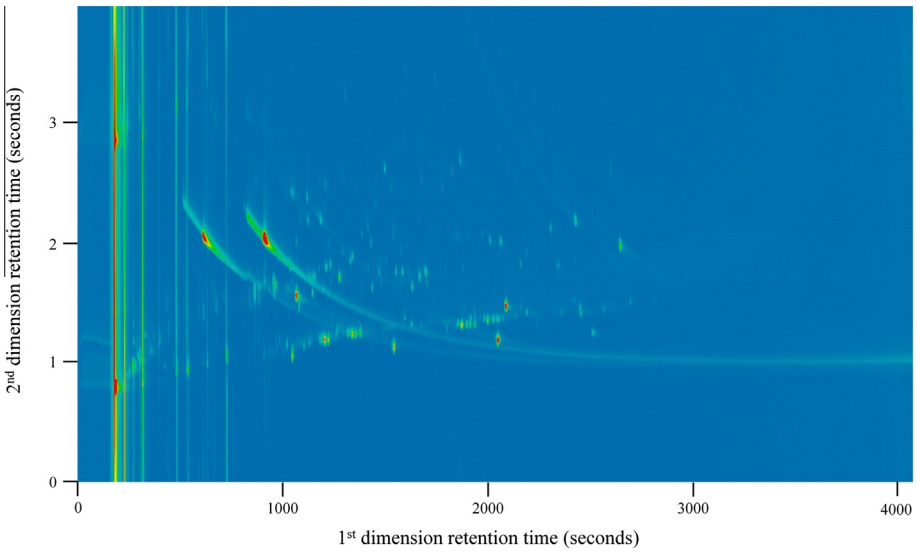

Fig. 3. Two-dimensional contour plot (chromatogram) of the West Texas cave sample.

thermal modulator being insufficient to trap the compound and thus the compound breaks through the modulator and this streak of signal is seen across the entire second dimension.

Some advantages provided by GC×GC which can be illustrated from Fig. 3 are increased chromatographic resolution, peak capacity, and signal-to-noise ratios. Increases in chromatographic resolution and peak capacity somewhat go hand-in-hand as chromatographic resolution and peak capacity are increased with orthogonal separations (separations over two dimensions).

The second sample was taken from a cave near San Antonio, Texas, called Robber Baron Cave. The two-dimensional contour plot (chromatogram) resulting from analysis of the sample on the MBST with the GC×GC is displayed in Fig. 4. Likewise, there is much complexity in this sample showing an average of 146 signals above an S/N threshold of 500 for the triplicate experimental runs.

In order to display the chromatographic complexity of the two cave samples a similar figure is displayed for background air sampled from within the laboratory. Sampling was performed in the exact same manner as the cave samples and the result is shown in Fig. 5. At the same S/N threshold of 500, only 1/3 the number of chromatographic signals are seen (approximately 50). These cave samples show much increased complexity in the number and intensity of the chromatographic signals present.

Another analytical advantage of GC×GC is chemical family recognition in terms of chromatographic space. A contour plot resulting from a standard GC×GC solution test mixture run on a Leco Pegasus® 4D GC×GC-TOFMS instrument housed in a separate division at Southwest Research Institute is displayed in Fig. 6. There are 49 signals numerically labeled in the contour plot and the chemical identity of said signals is listed in Table 2. On the basis of chemical identity (structure), signals are grouped and classified into similar chemical families denoted by the white oval regions in Fig. 6. Groupings of chemical families are denoted as aliphatics (alkanes, alkenes, and substituted alkanes and alkenes), mono-aromatics, polar aromatics, di- and tri-aromatics, and higher order aromatics (>tri-aromatics). The individual chemical identities in relation to their respective chemical family can be checked from Table 2. This chemical family recognition in the two-dimensional contour plot is one of the advantages of GC×GC and can be used as a screening tool for what types of chemical compounds are

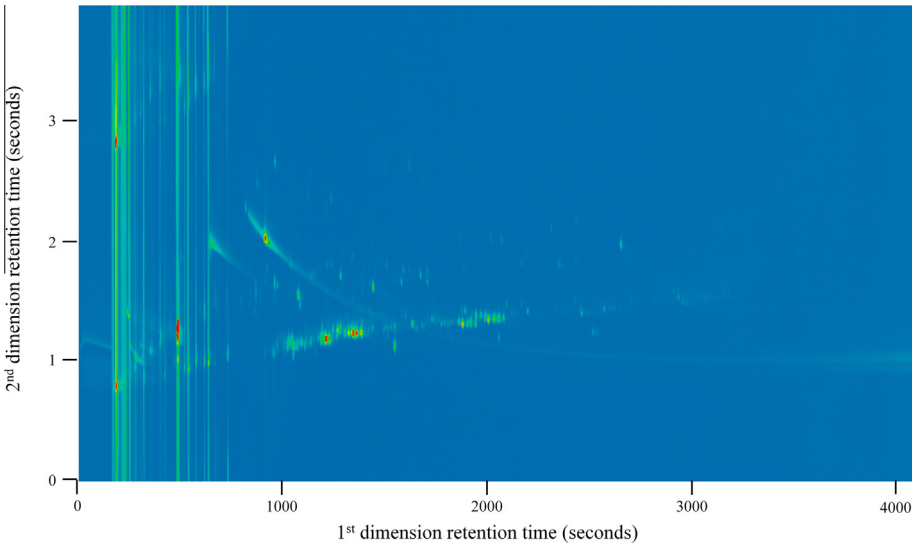

Fig. 4. Two-dimensional contour plot (chromatogram) of the Robber Baron cave sample.

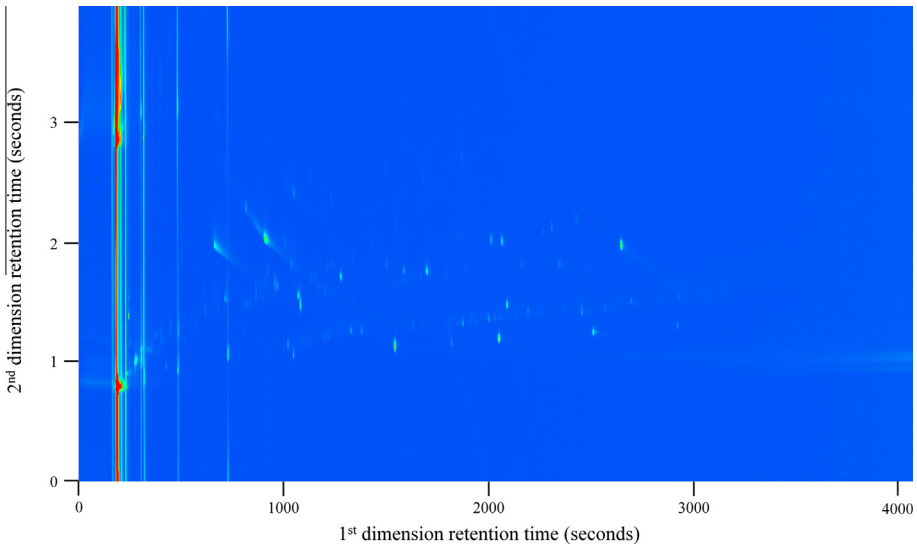

Fig. 5. Two-dimensional contour plot (chromatogram) of the background laboratory air sample.

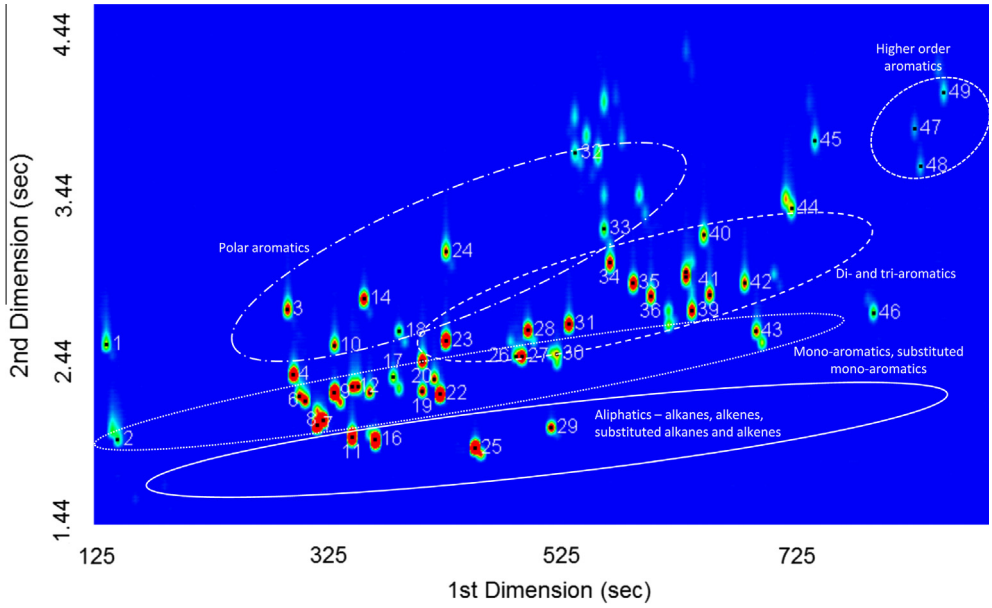

Fig. 6. Contour plot showing results from a GC×GC solution test mixture ran on a commercial Leco Pegasus® 4D GC×GC-TOFMS.

present in an unknown sample. For confident chemical identification, however, a mass spectrometer such as the time-of-flight mass spectrometer in the Pegasus® 4D GC×GC-TOFMS is required. At the time of this work, the Leco Pegasus® 4D GC×GC-TOFMS was unavailable for use.

Using the contour plot of Fig. 6 and Table 2 of chemical compounds as a guide, some of the chemical families are denoted in Fig. 7. This comparison is valid as the two instruments used the same column configurations (nonpolar volatility based first dimension separation and polar second dimension separation), oven temperature ramps, etc. The differences in liquid injection versus desorption from the MBST are minimal and the resulting retention times of components may vary slightly but the groupings of components in chemical families (chemical family recognition) still holds. The chemical family groupings can be used in comparing the two cave samples as one can see some of the similarities and differences in the caves as well as seeing what 'types' of signals are present. In the comparative two-dimensional chromatograms part of the first dimension retention time has been truncated (does not go out to 4060 s as in Figs. 3 and 4) as the majority of the chromatographic signals elute in the first 3000 s.

Utilizing the compare feature in ChromaTOF® software allows a retention time matching in both the first and second dimension that can be used to determine like signals between the two chromatograms being compared. Filters are manually set to make the comparison and are as follows: first dimension retention time deviation from centroid of chromatographic signal of 4 s, second dimension retention time deviation of 0.1 s, and no filter for peak area or peak height as intensities for matching components might vary between samples. Applying these filters, the average number of matches between the triplicate experiments is 50 chromatographic signals (for comparative purposes, the number of matches between triplicate runs of the West Texas cave sample is on average ~125). One can look at Fig. 7 and visually see a few matching signals but the chromatographic complexity requires the software to hunt for all of the like signals. Many of the matching signals are

Table 2
List of chemical compounds detected in the GC×GC solution test mixture.

Peak number	Chemical compound	Peak number	Chemical compound	Peak number	Chemical compound
1	*N*-Nitrosodimethylamine	18	Phenol, 2-nitro-	35	Acenaphthene
2	Pyridine	19	Phenol, 2,3-dimethyl-	36	Dibenzofuran
3	Aniline	20	Methane, bis(2-chloroethoxy)-	37	Fluorene
4	Bis(2-chloroethyl) ether	21	Phenol, 2,5-dichloro-	38	Diethyl phthalate
5	Phosphonic acid, (*p*-hydroxyphenyl)-	22	Benzene, 1,2,4-trichloro-	39	Naphthalene, 2-methyl-
6	Phenol, 2-chloro-	23	Azulene	40	Diphenylamine
7	Benzene, 1,3-dichloro-	24	*m*-Chloroaniline	41	Azobenzene
8	Benzene, 1,2-dichloro-	25	1,3-Butadiene, 1,1,2,3,4,4-hexachloro-	42	Diphenyl ether
9	Benzene, 1,4-dichloro-	26	Phenol, 4-chloro-3-methyl-	43	Benzene, hexachloro-
10	Benzyl alcohol	27	Naphthalene, 1-methyl-	44	Phenanthrene
11	Isopropyl alcohol	28	Naphthalene, 1-methyl-	45	Carbazole
12	Phenol, 3-methyl-	29	1,3-Cyclopentadiene, 1,2,3,4,5,5-hexachloro-	46	Dibutyl phthalate
13	1-Propanamine, *N*-nitroso-*N*-propyl-	30	Phenol, 2,4,5-trichloro-	47	Fluoranthene
14	Benzene, nitro-	31	Naphthalene, 1-chloro-	48	Pyrene
15	Phenol, 3-methyl-	32	*o*-Nitroaniline	49	Fluoranthene
16	Ethane, hexachloro-	33	Dimethyl phthalate		
17	2-Cyclohexen-1-one, 3,5,5-trimethyl-	34	Biphenylene		

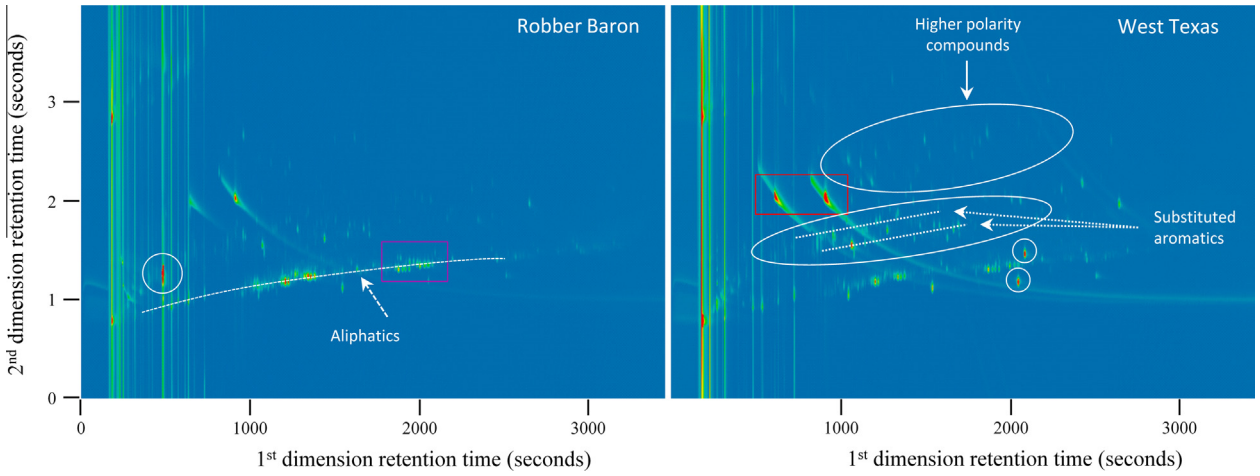

Fig. 7. Comparison of the two-dimensional chromatograms from the two cave samples with some of the more noticeable differences in detected components as well as denoted regions specific to chemical families for a screening tool of what 'type' of components are present in the caves.

seen in the aliphatic (branched and linear alkanes, alkenes, etc.) trend line and areas around the substituted aromatics. Two of the most noticeable similar signals are more polar compounds at a second dimension retention time around 2 s (marked by the dark red box in the right of Fig. 7). The same signals are seen in the figure at left but at significantly different abundances from the colors of the contour plot. There are also many matches among the smaller alkanes where streaking of the signal is seen across the entire second dimension.

Those signals that are not among the 50 matches are unique signals to the respective samples (88 and 96, respectively from the 138 and 146 chromatographic signals originally above an S/N threshold of 500). A few of the more noticeable unique signals are denoted in Fig. 7. The first signal is marked by the white circle in the lower left portion of the Robber Baron cave sample at left of Fig. 7 around a first dimension retention time of 500 s and a second dimension retention time of 1.2 s. In the plot at right (West Texas cave sample), a similar signal is seen but at a second dimension retention time around 1 s (following the aliphatic trend line). The deviation in this signal from the Robber Baron sample shows increased polarity and would be an interesting signal to target with mass spectrometry detection employed. The second set of differences take place along the aliphatic trend line at a first dimension retention time around 2000 s denoted by the purple box in the left plot (Robber Baron sample). Within the region defined by the purple box, there are an increased number of signals (3) sitting just above the dotted white line representing the aliphatic trend line. These signals are not present in the West Texas cave sample. In the same region, two very distinct signals present in the West Texas cave sample denoted by the two small white circles in plot at right are not present in the Robber Baron sample. These two signals are very abundant and one deviates above the trend line (more polar) while the other is below the trend line (less polar). The last set of unique signals are seen in the West Texas cave sample denoted by the large white oval for the highly polar compounds in the region of second dimension retention time of 2–3 s. These unique sets of signals between the two samples would be interesting starting points for mass spectrometry detection and identification to help characterize the chemical differences between the caves and what could be responsible for said differences.

A better, more visually striking, comparison can be made using the subtract tool in the ChromaTOF® software. The software allows the user to select two contour plots and subtract one of the contour plots from the other and one can more easily see the variation in both signal intensity and unique signals between the two samples. This comparison was done for both cave samples and the results are presented in Fig. 8. The lower plots in Fig. 8 represent the subtraction of one contour plot from another and the resulting contour

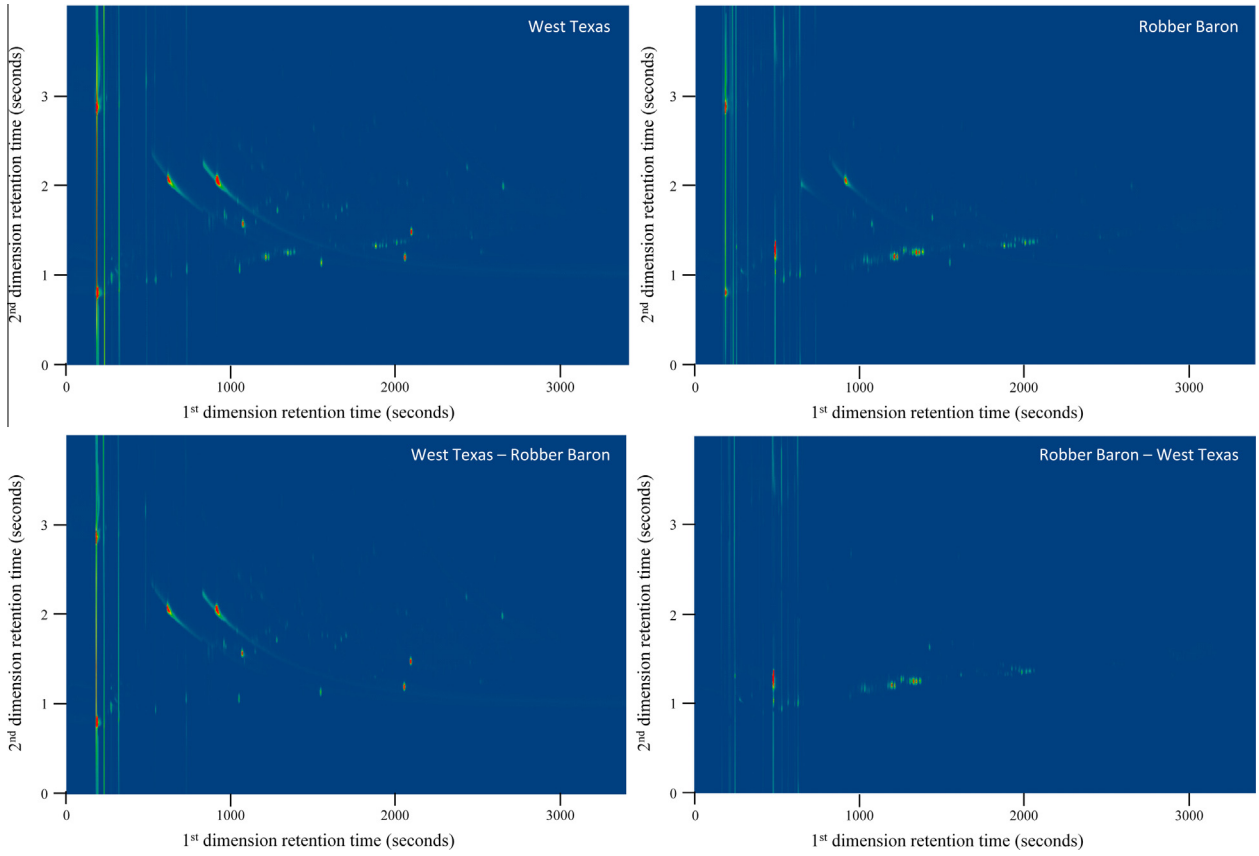

Fig. 8. Comparison of the two cave samples utilizing the subtract tool in the ChromaTOF® software. The upper left contour plot shows the raw data of the West Texas cave sample while the lower left plot depicts said contour plot minus the raw data of the Robber Baron cave sample. The plots at right are for the initial Robber Baron cave sample and subtraction with the compared sample.

plots provide greater visual acuity in the differences of the cave atmospheres.

4. Conclusion

Our cave sampling method coupled with sample pre-concentration using a multi-bed sorption trap (MBST) prior to injection onto a commercial GC×GC-FID has proven to be a successful tool for screening, fingerprinting, and comparing cave atmospheres. Results from two different Texas caves compared to a background air sample from within a laboratory (normal building environment) show variation in volatile and semi-volatile compounds. Furthermore, the two caves show differences in chromatographic signals and more specifically differences in the amount and abundance of signals corresponding to different chemical families (i.e. suspected aliphatics, aromatics, polar compounds, etc.). To improve upon the method in the future, mass spectrometry detection will be implemented with the commercial GC×GC instrument. Effluent will be diverted through a heated transfer line into an electron impact source and ions will then be extracted from the source into a time-of-flight mass spectrometer. However, it should be reiterated that the power of GC×GC for providing chemical information for differentiating and fingerprinting atmospheres can be seen without the use of a mass spectrometer and can be used to glean information about likeness and diversity of atmospheres.

Conflict of interest

There is no conflict of interest for any of the authors of this work.

Acknowledgements

The authors would like to acknowledge the property owner of the West Texas cave for access and sampling of the cave. The authors would also like to thank Southwest Research Institute and the Presidential Internal Research Grant #R8223 for funding this research.

References

[1] D.S. Jones, H.S. Albrecht, K.S. Dawson, I. Schaperdoth, K.H. Freeman, Y. Pi, A. Pearson, J.L. Macalday, Community genomic analysis of an extremely acidophilic sulfur-oxidizing biofilm, ISME J. 6 (2012) 158–170.
[2] L.D. Hose, J.A. Pisarowcz, Cueva de Villa Luz, Tabasco, Mexico: reconnaisance study of an active sulfur spring cave and ecosystem, J. Cave Karst Stud. 61 (1999) 13–21.
[3] G. E. Cushing, T. N. Titus, J. J. Wynne, P. R. Christensen, THEMIS observes possible cave skylights on Mars, in: Lunar and Planetary Science Conference XXXVIII, 2007.
[4] D.S. Blehert, A.C. Hicks, M. Behr, C.U. Meteyer, B.M. Berlowski-Zier, E.L. Buckles, J.H. Coleman, S.R. Darling, A. Gargas, R. Niver, J.C. Okoniewski, R.J. Rudd, W.B. Stone, Bat white-nose syndrome: an emerging fungal pathogen?, Science 323 (2009) 227
[5] J. Foley, D. Clifford, K. Castle, P. Cryan, R.S. Ostfeld, Investigating and managing the rapid emergence of white-nose syndrome, a novel, fatal, infectious disease of hibernating bats, Conserv. Biol. 25 (2011) 223–231.
[6] A.M. Minnis, D.L. Lindner, Phylogenetic evaluation of *Geomyces* and allies reveals no close relatives of *Pseudogymnoascus destructans*, comb. nov., in bat hibernacula of eastern North America, Fungal Biol. (2013), http://dx.doi.org/10.1016/j.funbio.2013.07.001.
[7] A. Froschauer, J. Coleman, North American bat Death Toll Exceeds 5.5 Million from White-Nose Syndrome, U.S. Fish and Wildlife Service, Office of Communications, 2012.
[8] D.E. Northup, L.A. Melim, M.N. Spilde, J.J. Hathaway, M.G. Garcia, M. Moya, F.D. Stone, P.J. Boston, M.L. Dapkevicius, C. Riquelme, Lava cave microbial

communities within mats and secondary mineral deposits: implications for life detection on Mars, Astrobiology 11 (2011) 601–618.
[9] R.J. Léveillé, S. Datta, Lava tubes and basaltic caves as astrobiological targets on Earth and Mars: a review, Planet. Space Sci. 58 (2010) 592–598.
[10] J. N. Mitchell, E. J. Mitchell, Airflow and CO_2 in Robber Baron Cave, in: Proceedings of the 15th International Congress of Speleology, Kerrville, Texas, 2009.
[11] E.L. Patrick, K.E. Mandt, E.J. Mitchell, J.N. Mitchell, K.N. Younkin, C.M. Seifert, G.C. Williams, A prototype mass spectrometer for in situ analysis of cave atmospheres, Rev. Sci. Instrum. 83 (2012) 105116.
[12] D.S. Blehert, J.M. Lorch, A.E. Ballmann, P.M. Cryan, C.U. Meteyer, Bat white-nose syndrome in North America, Microbe 6 (2011) 267–273.
[13] G. Schomburg, Two-dimensional gas chromatography: principles, instrumentation, methods, J. Chromatogr. A 703 (1995) 309–325.
[14] W. Bertsch, Two-dimensional gas chromatography. Concepts, instrumentation and applications – part 1: fundamentals, conventional two-dimensional gas chromatography, selected applications, J. High Resolut. Chromatogr. 22 (1999) 647–655.
[15] W. Bertsch, Two-dimensional gas chromatography. concepts, instrumentation, and applications – part 2: comprehensive two-dimensional gas chromatography, J. High Resolut. Chromatogr. 23 (2000) 167–181.
[16] Z. Liu, J.B. Phillips, Comprehensive two-dimensional gas chromatography using an on-column thermal modulator interface, J. Chromatogr. Sci. 29 (1991) 227–231.
[17] G.S. Frysinger, R.B. Gaines, E.B. Ledford, Quantitative determination of BTEX and total aromatic compounds in gasoline by comprehensive two-dimensional gas chromatography (GC×GC), J. High Resolut. Chromatogr. 22 (1999) 195–200.
[18] G.S. Frysinger, R.B. Gaines, Determination of oxygenates in gasoline by GC×GC, J. High Resolut. Chromatogr. 23 (2000) 197–201.
[19] J.M. Dimandja, A new tool for the optimized analysis of complex volatile mixtures: comprehensive two-dimensional gas chromatography/time-of-flight mass spectrometry, Am. Lab. 2 (2003) 42–53.
[20] P. Marriott, R. Shellie, J. Fergues, R. Ong, P. Morrison, High resolution essential oil analysis by using comprehensive gas chromatography methodology, Flavour Fragrance J. 15 (2000) 225–239.
[21] K. Ralston-Hooper, A. Hopf, C. Oh, X. Zhang, J. Adamec, M.S. Sepulveda, Development of GC×GC/TOF-MS metabolomics for use in ecotoxicological studies with invertebrates, Aquat. Toxicol. 88 (2008) 48–52.
[22] R.E. Mohler, K.M. Dombek, J.C. Hoggard, E.T. Young, R.E. Synovec, Comprehensive two-dimensional gas chromatography time-of-flight mass spectrometry analysis of metabolites in fermenting and respiring yeast cells, Anal. Chem. 78 (2006) 2700–2709.
[23] W. Welthagen, R.A. Shellie, J. Spranger, M. Ristow, R. Zimmermann, O. Fiehn, Comprehensive two-dimensional gas chromatography-time-of-flight mass spectrometry (GC×GC-TOF) for high resolution metabolomics: biomarker discovery on spleen tissue extracts of obese NZO compared to lean C57BL/6 mice, Metabolomics 1 (2005) 65–73.
[24] J. Dalluge, L.P. van Stee, X. Xu, J. Williams, J. Beens, R. Vreuls, U.A. Brinkman, Unravelling the composition of very complex samples by comprehensive gas chromatography coupled to time-of-flight mass spectrometry: cigarette smoke, J. Chromatogr. A 974 (2002) 169–184.
[25] H.J. De Geus, I. Aidos, J. de Boer, J.B. Luten, U.A. Brinkman, Characterisation of fatty acids in biological oil samples using comprehensive multidimensional gas chromatography, J. Chromatogr. A 910 (2001) 95–103.
[26] M. Libardoni, J.H. Waite, R. Sacks, Analysis of human breath samples with a multi-bed sorption trap and comprehensive two-dimensional gas chromatography (GC×GC), J. Chromatogr. B 842 (2006) 13–21.
[27] L. Mondello, P.Q. Tranchida, P. Dugo, G. Dugo, Comprehensive two-dimensional gas chromatography-mass spectrometry: a review, Mass Spectrom. Rev. 27 (2008) 101–124.
[28] H.J. Cortes, B. Winniford, J. Luong, M. Pursch, Comprehensive two dimensional gas chromatography review, J. Sep. Sci. 32 (2009) 883–904.
[29] A. McCarrick, Long term storage of air samples - a study of two bag materials, SAE Technical Paper, 2000–01-2502, 2000, http://dx.doi.org/10.4271/2000-01-2502.
[30] J.M. Sanchez, R.D. Sacks, On-line multibed sorption trap and injector for the GC analysis of organic vapors in large-volume air samples, Anal. Chem. 75 (2003) 978–985.
[31] J.M. Sanchez, R.D. Sacks, GC analysis of human breath with a series-coupled column ensemble and a multibed sorption trap, Anal. Chem. 75 (2003) 2231–2236.